

**The Hyden Fault Scarp, Western Australia:
Palaeoseismic Evidence For Repeated Quaternary
Displacement In An Intracratonic Setting**

Running title: Hyden palaeoseismic study

Dan Clark¹, Mike Dentith², Karl-Heinz Wyrwoll², Lu Yanchou³, Victor Dent² &
William Feartherstone⁴

1. Geoscience Australia, GPO Box 378 Canberra ACT 2601. dan.clark@ga.gov.au
2. School of Earth & Geographical Sciences, the University of Western Australia, Crawley WA 6009.
3. Institute of Geology, China Seismological Bureau, Beijing, China.
4. Western Australian Centre for Geodesy, Curtin University of Technology, Bentley, WA

Abstract

We present new paleoseismicity data for the 30 km long and 2.5 m high Hyden fault scarp in Western Australia, which, when combined with the results of previous research, provides the most extensive record of surface rupturing earthquakes yet assembled for an "active" Australian intracratonic fault. The data indicate that four to five surface rupturing earthquakes have occurred on the Hyden Fault during the Quaternary (E1: ca. 20 ka, E2: ca. 50-55 ka, E3: ca. 100 ka, and two events E4 and E5, >200 ka). Activity is episodic, with single seismic cycle slip rates varying from 0.03 mm/yr to less than 0.01 mm/yr. Palaeo-earthquake magnitudes are estimated to have been in the order of M 6.8. The identification of a similar fault scarp immediately northwest of the Hyden scarp, and of two air-photo lineaments to the west of the Hyden scarp, all underlain by faults imaged using high-resolution geophysical data, indicates that strain is distributed amongst a family of faults in this region. The presence of multiple faults indicates that the seismic hazard at any given location is likely to be appreciably greater than the hazard posed by a single fault considered in isolation.

Keywords:

Hyden, palaeoseismology, Quaternary, seismicity, Western Australia

Introduction

Australia is considered to be a stable continental region (SCR, Johnston et al., 1994), yet large and potentially damaging ‘intra-plate’ earthquakes are not uncommon. Seismicity occurs across most of the continent with a possible association between zones of greater activity and the margins of major geological entities (Denham, 1988; Dentith & Featherstone, 2003). Between twenty and thirty earthquakes of magnitude six or more are known from approximately two hundred years of observation (McCue, 1990; Clark & McCue, 2003; **Fig. 1**), and at least five of these events have been sufficiently large and shallow to produce a fault scarp at the surface (e.g. McCue, 1990 and **Fig.1**).

This contribution describes palaeoseismic evidence for repeated rupture on an historically aseismic fault zone located approximately 350 km east of Perth, close to the town of Hyden, in Western Australia (**Fig. 2**). The largest fault in the area coincides with a distinct scarp, which can be traced for about 30 km (Chin et al., 1984). It is noteworthy that the scarp occurs well to the east of the current zone of seismic activity (**Fig. 2**). In a companion paper, the geophysical characteristics of the scarp are described, leading to the recognition that it coincides with one of several basement faults whose history extends back to the Precambrian.

An understanding of the age and characteristics of the pre-historic seismicity represented by the fault scarps leads to an improved understanding of earthquake-prone areas of the recent geologic past, and with this brings the potential for the assessment of seismic hazard in this region of Western Australia.

Regional Seismicity and Stress Field

Over at least the last 40 years the southwestern part of Western Australia has been one of the most seismically active regions in Australia (**Figs. 1 & 2**). Doyle (1971) designated the area encompassing the most dense population of epicentres the Southwest Seismic Zone (SWSZ). Though most earthquakes are relatively small, the SWSZ has been host to three of the five known historic surface rupturing earthquakes; 1968 - Ms 6.8 Meckering and 1970 – Mb 5.7 Calingiri (Gordon & Lewis, 1980) and 1979 - Ms 6.0 Cadoux (Lewis et al., 1981).

In addition to the three fault scarps caused by historic events, there are a number of ancient fault scarps in the region (McCue, 1990). The general northerly trend of these scarps is consistent with their formation under conditions similar to the contemporary crustal stress field, which has a horizontal maximum principal stress oriented roughly east-west (Hillis & Reynolds, 2000; Clark & Leonard, 2003). This stress regime encourages reverse faulting on structures trending north-south. It is estimated that the Australian crustal stress field established itself in the current configuration in the late Miocene - early Pliocene (Sandiford, 2003a).

Geology and Geomorphology

The bedrock geology of the Hyden area comprises Archaean granitoids intruded by Proterozoic mafic dykes. A greenstone belt occurs some tens of kilometres to the east and there are localised occurrences of greenstone belt-type supracrustal rocks within the granitoids. Exposure is extremely poor due to pervasive weathering and an extensive Quaternary, largely eolian sand cover. Consequently, only reconnaissance geological mapping, at 1:250,000 scale has been completed (Chin et al., 1984)

The geomorphology of the Hyden area is characterised by very gently undulating topography. Hills are typically granitic and are locally capped with laterite. Valley floors denoting palaeodrainage lines, possess more more younger aeolian and alluvial infills. Valley slopes comprise sandy plains, subdued granitic outcrops, colluvial material and ferruginous lateritic duricrust. The sandplain deposits are up to 3-4 m deep and are thought to have been derived from deeply weathered profiles, and generally have only been transported short distances from source (Chin et al., 1984). Locally, the sand plain has been partially removed leaving dissected etchplain, which consists of remnant sandplain and remnant deeply weathered profiles.

Palaeoseismological Investigations of the Hyden fault Scarp

Scarp Morphology

The Hyden scarp was recognised in the course of regional mapping (Chin et al., 1984), and is indicated as an approximately 30 km long north-south trending scarp, separating into two strands in its central section. Detailed analysis of aerial photographs has revealed a more complicated pattern of faulting. (**Fig.3a**). The central bifurcation is found to comprise an area where northern and southern strands of the fault overlap, with associated linking and sub-parallel faults. At its southern end the fault scarp changes trend and is represented by a series of sub-parallel lineaments. To the west there are two sub-parallel lineaments which are likely to be associated with faulting. A detailed digital terrain model (10m resolution, <http://www.landmonitor.wa.gov.au>) shows the Hyden scarp, plus a second more

degraded scarp to the west, which lies on the northward continuation of the more westerly of the aerial photo lineaments (**Fig.3b**).

Previous Investigations

In 1982 the Australian Geological Survey Organisation (AGSO) in conjunction with the Geological Survey of Western Australia excavated three narrow trenches across the main Hyden fault scarp (herein denoted the AGSO north, centre and south trenches, **Fig. 3b**). Carbonaceous materials collected from a pond near the fault, thought to have been formed as the result of defeat by faulting of westerly flowing drainage, yielded inconclusive radiocarbon ages. Palaeomagnetic and palynological investigations were similarly unsuccessful in determining the age of faulting. The logs of the trench walls have subsequently been lost.

In 1997 the Hyden fault scarp was again investigated by members of the United States Geological Survey (Crone et al., 2003) The trench excavated in the course of their investigation is referred to as the USGS trench. Data from the study indicate that two surface-faulting earthquakes occurred on the Hyden fault in the late Quaternary, at ca. 30 ka and ca. 50-55ka. The authors contend that these events were preceded by no surface faulting at their trench site for at least several hundred thousand years and possibly one million years or more. The conclusion was based upon the observation that pre-penultimate event fault strands within the hangingwall duricrust have no topographic expression. This history was taken to define an episodic pattern of faulting for the Hyden fault in which relatively short periods of activity are separated by long periods of quiescence, similar to the patterns described for other SCR faults (e.g. Crone et al., 1997).

Both late Quaternary events resulted in the formation of a minimum of 80 cm of vertical displacement, indicating that the causal events were comparable in size (Crone et al., 2003). The maximum vertical displacement that may be shared between the two events, assuming no displacement inherited from previous events, is given by the 2.6 m offset in the bedrock at the site. It is not clear from these data what proportion of the scarp ruptured during each event. However, relationships developed between scarp height, length and earthquake magnitude (Wells & Coppersmith, 1994) suggest that events in the order of M 6.5-6.7, generating scarps of length 15-25 km, are consistent with the possible range of vertical offsets (80 – 130 cm).

The apparent sense of displacement across the steeply east dipping late Quaternary fault traces in the Crone et al. (2003) trench is normal-oblique. This contrasts with the apparent reverse displacement across the moderately west-dipping pre-penultimate event fault traces, and is contrary to that which might be expected under conditions imposed by the contemporary stress field. Crone et al. (2003) do not directly address this inconsistency, and while finding no compelling geomorphic evidence to indicate a direction of lateral slip (such as consistently offset drainage channels), maintain that the overall expression of the fault, particularly the linearity of the trace of the scarp over 30 km, is suggestive of a significant lateral-slip component to displacement. However, modelling conducted as part of the present study shows that the terrain around Hyden is so subdued that planar features with dips of as little as 10° intersect the ground surface along a linear trace. The implication that the linear trace is suggestive of strike-slip is thus equivocal.

New Palaeoseismological Data

The Hyden Fault was revisited in 2001 with the principal aims of: (1) reconciling the apparent normal offsets identified in the USGS trench with the reverse structures also identified in the trench, and with the contemporary stress field; and (2) attempting to provide time constraint on reverse displacements on the fault. In addition to geophysical surveys described elsewhere, the study involved excavation of a trench across the fault scarp. Optically stimulated luminescence (OSL) dating was undertaken on selected samples from the trench.

Description of Trench Stratigraphy

A 36 m long and 4 m deep trench was excavated at the location of the AGSO south trench, 4 km to the south of the USGS trench (**Fig. 3b**). The fault scarp at this location has a relatively modest topographic expression, occurring as a shallow rise no more than a couple of metres in height. The trench exposes a series of westerly dipping faults within a succession comprising intensely weathered *bedrock* overlain by unconsolidated clastic sediments (**Fig.4**).

The stratigraphy of the up-thrown western side of the fault zone (hangingwall block) comprises a deeply weathered profile dissected by faulting. The lowermost identified unit (Unit 6) comprises strongly banded ferricrete. The rock consists of alternating pale sandy/clayey bands and reddish silicified and ferruginised bands. The reddish bands are composed of cemented sand and associated quartz clasts that typically appear rounded and range up to about a centimetre in diameter.

The basal unit is overlain by weakly banded to massive partly pisolitic ferricrete (Unit 5), developed in sand–mud sediment. Banding is defined by pale, indistinct and discontinuous clay-dominant layers.

Unit 5 is very similar in character to the lowermost unit exposed in the footwall block; Unit 4-2. However, no definite correlation across the fault zone could be made as no prominent marker horizons were identified. The contact between Unit 4-2 and overlying massive to very weakly banded ferricrete (Unit 4-1) is gradational, and is difficult to distinguish. The units are separated on the basis that large transported clasts, typically of banded iron formation or other iron rich lithology (up to 10 cm in diameter), are present in Unit 4-1, but not in 4-2. The ferricrete clasts are clearly hosted in a older sediment body.

Proximal to faults F2 to F5 the ferricrete is strongly sheared and disaggregated, and readily spalled from the trench wall following excavation. East of fault trace F2 the weak banding in Unit 4-2 has been arched upwards, producing a cavity. As these features all occur in the footwall of a major fault strand, they are interpreted to relate to disruption of the competent ferricrete strata during faulting. In the strongly fractured and altered region near F4, the ferricrete contains a relatively higher clay content. This characteristic is interpreted to reflect fracturing during faulting increasing the rock mass permeability and allowing access of groundwater, which subsequently resulted in enhanced chemical weathering. Clayey seams of around one centimetre thick located along the fault trace F3 are similarly ascribed to enhanced weathering subsequent to faulting.

A series of parallel, sub-vertical, north-trending in-filled fissures occur on both sides of the fault zone, transecting Units 4, 5 & 6. These structures are up to 10 cm wide and contain colluvial material comprising pisolites held in a yellow sand matrix. In some instances planar pebbles appear vertically aligned within the structures, suggesting that they fell into an open fissure. The structures are therefore interpreted to be tension fissures related to monoclinical warping of the ferricrete layer during faulting.

Several vertical sand-filled 'pipes' occur within the ferricrete profile, most prominently in the footwall block (e.g. at 2 & 16 m on the horizontal scale). These were particularly noticeable in the trench floor, where they were exposed in cross section as roughly circular. The pipes are typically filled with medium grained pale white sand containing iron-rich nodules and concretions similar to those found in the surrounding ferricrete. These features are interpreted as marking former large tree roots. Unit 4-3 is a cobbly gravel that is strongly iron oxide cemented. Platey ferricrete cobbles are in places sub-vertically aligned within the unit suggesting a possible infill of large root structures. A fracture-fill origin related to faulting is discounted by the observation that weak lateritic banding passes undisturbed across the lower part of the feature. The ferricrete becomes partly disaggregated and nodular within a few centimetres of the interface with the overlying sandy units (Units 1 to 3), with locally more deeply weathered pockets.

East of fault trace F5 the ferricrete "bedrock" is buried beneath unconsolidated sandy deposits. The lowermost identified unit (Unit 3) is partly overlain by ferricrete bedrock that has been transported along F3. Thus, the deposition/formation of Unit 3

predates movement on fault F3. The unit is a sandy gravel comprising pea-sized ferricrete nodules (many with dark manganese oxide or iron oxide coatings) with an interstitial iron-stained medium-grained brown/red sand matrix. It is possible that the unit was part of a thin pisolitic soil covering the ground surface prior to faulting on F3. However, the wedge-like shape of the unit suggests the alternative that it may be slope colluvium or a colluvial wedge related to movement on faults F4 and/or F5.

Unit 3 is buried by a sequence of eastward thinning colluvial wedges (Unit 2) which truncate, and therefore postdate, faults F3 and F2. Five packages have been delineated within Unit 2. Unit 2-5 directly overlays a large block of ferricrete which is interpreted to relate to collapse of a free face following displacement on fault F3. The unit comprises a jumble of poorly-sorted randomly-oriented ferricrete cobbles set in a matrix of finer gravel and limonitic nodules. Medium grained yellowish sand fills the interstices. This context suggests that Unit 2-5 is a gravity deposit whose deposition closely post-dates reverse displacement along F3, and the collapse of the free face thus formed.

Units 2-1 to 2-4 overly Unit 2-5 and comprise sandy gravel (poorly sorted ferricrete clasts to 5-10 cm and nodules to 1 cm) proximal to the F2/F3 fault zones, grading laterally into well sorted, medium grained yellowish sand with a minor component of limonitic pebbles to the east. The prevalence of the gravely facies close to the fault strands suggest that the lenses represent gravity deposits and slope-wash colluvium derived from the eroding fault scarp. However, the predominance of well-sorted yellow sand, both in the gravel matrix, and distal to the fault trace F3, suggests an aeolian component within the wedges.

Unit 2 colluvium pinches out near the eastern end of the trench, and is absent above a high in the ferricrete bedrock associated with fault F1 (resulting from ~0.3 m of vertical slip). A lens of gravelly sand (Unit 2-4), similar in composition and appearance to Unit 2-3 colluvium, overlies bedrock in a depression in the ferricrete surface east of the trace of F1. Unit 2-4 also appears to be significantly younger than the sediment which mantled the ground surface prior to the deposition of Unit 2 colluvium (e. g Unit 3-1). On this basis we interpret the package to be a slope colluvium relating to relief generation across either fault F1 or F2/F3. Two explanations present themselves; either a faulting event on F1 pre-dates the deposition of Unit 2 materials (i.e. deposition was restricted by the Unit 4-1 bedrock high), or faulting on F1 has locally uplifted Unit 2 colluvium and allowed it to be eroded off the Unit 4-1 bedrock high. If the former explanation is adopted, fault strand F1 could have accommodated displacement during the same event as F2 and F3, avoiding the need to appeal to an additional surface rupturing earthquake. This simplest explanation is preferred, and Unit 2-4 is tentatively correlated in time to Unit 2-3.

Unit 2 deposits are overlain by an extensive sheet of well-sorted, medium-grained yellow sand which is up to 1.5 m thick (Unit 1). Carbonaceous material occurs sporadically throughout the sand layer, with a weak A-horizon at the surface. This layer is between 5 and 10 cm thick and comprises medium-brown discoloured sand. Similar horizontal discoloured bands occur at intervals within the sand sheet. An apparent palaeosol occurs a third of the way up through the package (Unit 1-1/Unit 1-2 boundary). It can be traced more or less continuously from the eastern end of the trench to just beyond the 8 m mark, before being lost, presumably to erosion at the

time of deposition of the overlying sediments. Approximately 12 cm of relief is preserved in this boundary above fault trace F1, mimicking similar relief in the upper boundary of Unit 4-1. Assuming that the Unit 1-1/Unit 1-2 boundary is shallowly easterly-dipping west of the 8 m mark (as is the present ground surface), the contact should project between OSL sample sites HF-2 and HF-3. The trace of fault F1 continues through Unit 1-2, where it is defined by a planar discoloured band in the sand. The discoloured band terminates at the Unit 1-1/Unit 1-2 boundary, suggesting that this boundary was at the surface at the time of the most recent displacement event on fault F1.

Palaeoseismic Interpretation of Trench Stratigraphy

It is proposed that at least three earthquake events are responsible for the observed relationships between faults and stratigraphy in the trench (**Fig.5**). These are denoted the most recent event (MRE), the penultimate event (PE) and the tri-ultimate event (TE). Evidence for the oldest event (TE) is provided by displacements of the upper boundary of Unit 6 across fault strand F5 and the absence of Unit 6 east of F4. The minimum slip required to restore the top of the Unit 6 boundary to horizontal west of F4 is 1.2 m (**Fig.5f-g**). Rotation of ferricrete banding between F4 and F5 indicates that F4 accommodated slip during this event also. While this supposition is supported by the spatial distribution of the crush zone in the footwall blocks of both F4 and F5, there is no constraint on the slip magnitude on F4 during the TE as Unit 6 was not encountered east of F4. The minimum displacement required to restore the top of Unit 6 to the level of the trench floor east of F4 is 0.3 m. This displacement is tentatively assigned to the TE. As the total displacement across F4 might be very

much greater than 0.3 m, it is possible that this fault accommodated slip in an event older than the TE.

The retro-deformation analysis indicates that a gentle slope existed at the site of the scarp prior to the PE (**Fig. 6e**), providing potential broad constraint on the age of relief generation during the TE (ie. all relief had not been removed by erosion), and supporting the supposition that the Unit 3 gravely sand is a relict colluvial deposit relating to the TE. Mineral coatings on ferricrete nodules, and the presence of significant iron staining within Unit 3 suggests that this unit is at least significantly older than the overlying colluvial packages. It is probable that some of the tension fissures in the hangingwall block west of fault F5 also formed during the TE.

Deposits associated with the TE are buried by colluvium (Unit 2) relating to displacement on faults F2 and F3 during the PE. While the majority of PE displacement (~1.5 m is required to restore the pre-PE ground surface, roughly equivalent to the top of Unit 4-1 at this time, **Fig. 5d**) was accommodated on fault trace F3, rotation of Unit 4-2 ferricrete banding between F2 and F3 indicates that F2 also accommodated slip during this event. This displacement must have been small as the vertical western margin of Unit 4-3 does not appear to have been substantially offset.

The relationship between Unit 2-5 and the underlying collapsed portion of Unit 4-1 suggests that Unit 2 colluvium reflects the degradation of a single event scarp, rather than of a number of smaller event scarps. The stratigraphy evident in Units 2-1 to 2-3, is thus interpreted as denoting localised depositional events. Based upon the

minimal evidence for substantial chemical breakdown of the ferricrete bedrock at the trench site, and the great volume of the overlying Unit 1 sand sheet, we interpret the sand component of Unit 2 to be substantially aeolian in origin, rather than locally derived sheet wash from the exposed hanging wall of the scarp. It is postulated that ~0.2 m of the 0.3 m of identified vertical slip across fault trace F1 also occurred during the PE. It is probable that the tension fissures which cross-cut faults F4 and F5, and the tension fissures that occur in the hangingwall of fault F1 also formed during this event.

Subsequent to the degradation of the penultimate event scarp to form the Unit 2 gravelly colluvium, aeolian sand deposition became the dominant process in filling the topographic low to the east of the scarp (**Fig. 5c**). Approximately 50 cm of sand sheet deposition had occurred prior to the occurrence of the most recent event identified in our trench. During the MRE fault F1 extended through the Unit 1-2 sand sheet to the palaeo-ground surface. Fault F3 was also reactivated, with the trace breaking up through the collapse block on the scarp face into the Unit 2 colluvium. An upward-warping of the upper boundary of Unit 1-2 indicates approximately 12 cm of vertical displacement occurred across F1 during this event. While no marker beds exist within Unit 1 to define a displacement magnitude across F3 a 'bump' in the upper boundary of Unit 2-1 at the location of the fault is indicative of ≤ 10 cm of displacement. Geometric relationships indicate that the displacement sense on both faults during the MRE was reverse.

Optically Stimulated Luminescence (OSL) Geochronology: Timing of Palaeo-earthquakes

Sandy sediment samples from nine localities within the trench (**Fig. 4**) were collected for single-aliquot regenerative-dose (SAR) OSL dating of quartz grains. The results of the analyses are presented in **Table 1**. Analytic procedures are presented in **Appendix 1**.

An attempt was made to place quantitative age constraint on the TE by sampling pebbly sand from Unit 3-1 (HF-5), and pebbly colluvium from a filled tension fissure interpreted to have formed during the TE (HSF-9) (**Fig. 4**). Both samples were saturated with respect to their OSL signal, indicating deposition ages of >200 ka.

Two OSL samples (HF-4 & HF-6) were taken from within 20 cm of the base of the lower colluvium relating to the PE (Unit 2-3; **Fig. 4**). The samples returned statistically indistinguishable OSL ages of approximately 90 ka (**Table 1**). As both samples were taken from the slope-wash/aeolian facies of Unit 2-3, a significant period of time may have elapsed between the building of relief and the deposition of the layer, perhaps as much as 5-10 kyr (cf. Crone et al., 2003). We therefore suggest that the PE probably occurred *ca.* 95 -100 ka.

Three laterally separated samples from close to the base of the Unit 1-2 sand sheet yielded OSL ages of 65.7 ± 2.9 ka, 68.5 ± 2.1 and 72.6 ± 2.3 ka, providing a maximum bound for the most recent faulting event to be identified in our trench. The oldest unfaulted strata above the MRE event horizon (EH1, **Fig. 4**) is dated by sample HF-2 at 40.3 ± 1.2 ka. The MRE therefore occurred in the interval between 40 and 70 ka.

The geochronological results do not provide unequivocal constraint on the timing of the first displacement event on fault trace F1, other than *ca.* 70 ka sands bury relief relating to the displacement. As Unit 2 colluvium proximal to F1 appears on sedimentological grounds to be much younger than unit 3-1, we consider it unlikely that the initial relief generation on F1 significantly pre-dates the PE. Alternatively, if the initial movement on fault F1 post-dates deposition of Unit 2 colluvium (i.e. Unit 2-4 is directly correlatable with Unit 2-3), then this additional faulting event must have occurred in the interval between the *ca.* 90 ka deposition of Unit 2-3, and the *ca.* 73 ka deposition of the overlying Unit 1-2 sand sheet. However, as previously mentioned it is simplest to suggest that F1 accommodated its initial ~0.2 m displacement during the PE *ca.* 95 -100 ka.

Discussion

Palaeoseismic History of the Hyden Fault

Paleoseismicity data from our study, and the study of Crone et al. (2003), have been compiled into a time-space diagram for comparison (**Fig. 6**). The data indicate that a minimum of four surface faulting earthquakes have occurred on the Hyden Fault in the late Quaternary (denoted E1-E4). Three events are constrained to have occurred in the last hundred thousand years, while the older event is most likely to be significantly greater than 200 kyr in age. Faulting at the location of our trench, in competition with erosion, has resulted in the preservation of approximately 2.6 m of vertical relief in the Tertiary ferricrete 'bedrock' (top of units 4-1 and 5-1) across all fault strands (**Fig. 4**). The lack of pre-Unit 3 colluvial deposits indicates that little

relief existed across the fault zone immediately prior to the E4 event (the TE in our trench). The observed displacement therefore largely relates to the three most recent events recognised in our trench (E2-E4).

We suggest that 0.2 m is a maximum estimate for the vertical relief produced in our trench during the E2 event (the MRE in our trench), based upon the limited displacement observed across post-E3, pre-E2 surfaces. A minimum estimate for the vertical displacement that occurred during the E3 event (our PE) on fault F3 is provided by the 0.8 m maximum thickness of the Unit 2 colluvial deposits. However, taking into account the volume of the wedge, and the displacement of the Unit 4-1 surface, the E3 event is likely to have produced around 1.2 m of vertical relief (~1.5 m total slip assuming dip slip motion) across this fault. We contend that trace F1 accommodated approximately 0.2 m of vertical slip during the E3 event also. The E4 event (TE in our trench) resulted in at least 1.2 m of slip (1.0 m vertical), as evidenced by the offset of the Unit 5/Unit 6 boundary west of F4. We tentatively assign the 0.3 m of vertical displacement required to bring the base of the trench level with the top of Unit 6 west of F4 to this event also.

Relationships developed between scarp height, length and earthquake magnitude (Wells & Coppersmith, 1994) suggest that events in the order of M 6.6-6.8 are consistent with the range of vertical offsets obtained for E3 and E4 (130 – 140 cm), and the 32 km scarp length. The total apparent vertical displacement across all fault strands is 2.9 m, which is commensurate with the offset in the ferricrete surface (2.6 m). This implies a perhaps unrealistic position where only 0.3 m of erosive lowering of the ferricrete surface in the hangingwall has occurred since E4. As it is unlikely

that the base of the trench east of F4 coincides exactly with the top of Unit 6, further displacement might be attributed to F4 during E4. Pre-E4 events across F4 are also possible.

A displacement in the ferricrete bedrock of similar magnitude was observed in the USGS trench. However, these authors' analysis suggests that the majority of relief generation at their location occurred during the E1 and E2 events (ca. 30 ka and ca. 50 ka respectively), which have no expression, and only minor expression, respectively, in our trench. Furthermore, the USGS trench log indicates that E1 and E2 involved dilation, rather than the compression that we observe. Faults bearing reverse geometry do exist in the Crone et al. (2003) trench. For example, their fault F1, which occurs midway down the scarp expressed in the Tertiary ferricrete (Crone et al., 2003, Fig. 7b), is very similar in context and appearance to our F4/F5. The authors did not consider this fault to have been active during late Pleistocene events, presumably based upon an absence of sharp relief and related colluvium overlying bedrock on the downthrown side of the F1 fault zone. However, the fluvial gravel unit overlying bedrock (Unit 4, Crone et al., 2003) allows that fluvial activity might have removed colluvium relating to events prior to E2 at this site (including *ca.* 90 ka colluvium), and potentially also modified the scarp. Based upon its location with respect to the relief in the ferricrete surface, and its geometry, we tentatively correlate the event that formed this fault with displacement on our F4/F5 faults during E4 (**Fig. 6**). While it is possible that slip also occurred on this fault during E3, which has the greatest vertical displacement in our trench, no sedimentological evidence to support an association was reported by Crone et al., (2003).

The oldest reverse fault traces in the USGS trench occur near the westernmost end of the trench, and are not associated with relief. Hence, the formation of these fault strands is broadly assigned to a pre-E4 event (E5), of indeterminate age (**Fig. 6**). Crone et al. (2003) suggest that the faults may have formed in the early Quaternary or late Tertiary. No direct correlatives for these faults were observed in our trench.

While it is to be expected that the magnitude of displacement will vary markedly along the length of a surface rupture (e.g. Hemphill-Haley & Weldon, 1999), potentially accounting for the absence of evidence for E3 in the USGS trench, explaining changes in displacement sense require more complex explanation. That the E2 rupture is compressive in nature in our trench indicates that it is unlikely that the crustal stress field switched to dilative sometime after 90 ka, before switching again to the present compressive state. The transition in the USGS trench from reverse (pre-E2) to normal (E1, E2) displacement is therefore most likely to relate to some geometric complexity in the rupture plane or interaction between faults. For example, the rupture progression in the USGS trench is from west to east, with younger reverse ruptures being progressively shallower than older ones. It is possible that further shallowing of the underlying reverse dislocation plane at depth during E2 and E1 caused dilation in the overlying brittle ferricrete. This would require that displacement from the reverse rupture was distributed in the near-surface materials without a discrete reverse fault trace forming. Alternatively, maturation of the structures linking the right step in the main fault just to the south of the USGS trench may have induced local subsidence.

The right hand column of **Fig. 6** presents slip rate data for the three complete seismic cycles for which we have age constraint. The slip rate for the youngest complete seismic cycle (E2-E1, ca. 50 - 30 ka, 0.03 mm/yr) is derived from the maximum thickness of the colluvial wedge relating to the E2 event (80 cm) in the Crone et al. (2003) trench. A similar slip rate of 0.03 mm/yr is obtained for the previous seismic cycle (E3-E2, 100 - 50 ka). As we have only a broad minimum age bound on the time of the E4 event (\geq 200 -250 ka), the slip rate of 0.01 mm/yr obtained for the E4 to E3 seismic cycle (100 - $>$ 200 ka) is a maximum estimate only. Irrespective, the estimate implies a marked change in rate from the two younger cycles. These data indicate highly episodic fault activity and variable slip rates on the Hyden Fault in the last several hundred thousand years, consistent with data obtained on intraplate faults elsewhere (e.g. Meers Fault Oklahoma, Crone & Luza, 1990; Cheraw Fault Colorado, Crone et al., 1997; Roopena Fault South Australia, Crone et al., 2003).

Implications for Seismic Hazard

The identification of several geologically recent fault scarps in the Hyden area indicates a susceptibility to large earthquake events under conditions imposed by the contemporary stress field, in turn implying hazard. The characteristics of the seismicity on the faults underlying these scarps have the potential to define, or at least constrain the hazard. The data from the trenched fault indicates episodic surface rupture with a frequency varying between of tens of thousands to hundreds of thousands of years (see also Crone et al., 2003). Even though events on the fault are likely to be sufficiently large ($M > 6$) to cause widespread damage to the surrounding rural communities, the calculated slip rates (< 0.01 to 0.03 mm/yr) are insufficient to significantly impact probabilistic hazard calculations for even critical infrastructure

(cf. Frankel et al., 1996; Stirling, 1998, 2002). However, evidence indicating that nearby faults have experienced surface rupture during the Quaternary suggests that the hazard at any given location is greater than the hazard posed by a single fault considered in isolation (e.g. Machette, 1998). If, for example, regional slip is distributed between the Hyden fault and the degraded scarp to the north, a doubling of the slip rate is conceivable. This value could be enhanced still further if slip on the lineaments several kilometres to the west of the fault, and the Quaternary scarp 30 km to the southwest (Fig. 1; Chin et al., 1984), are considered. Based upon the five lineaments discussed in this paper, the recurrence for large earthquakes in the Hyden region could be reduced by a factor of five, from tens of thousands of years to only a few thousand. Future studies might date events on all features in the Hyden region to test if the episodicity seen on individual faults relates to a regular recurrence of surface rupture on a family of nearby faults, or if the episodicity is characteristic of a larger area.

It is clear that modern seismic hazard assessments must use not only the catalogue of historic seismicity, but must also integrate data from a comprehensive inventory of Quaternary faults showing evidence for movement in a timeframe commensurate with an average seismic cycle on an intraplate fault (say 20,000 years to 100,000 years). Not only do Quaternary scarps locate the source location of potential future strong ground motion and more generally flag regions prone to large earthquake events, but the potential exists to at least semi-quantitatively assess the hazard posed by the largest events that might be expected in an area.

Conclusions

New palaeoseismicity data on the 32 km long and 2.5 m high Hyden Fault scarp, combined with the results of a previous study (Crone et al., 2003), provide the most extensive record to date of surface rupturing earthquakes on an Australian intraplate fault. The data indicate that four to five surface rupturing earthquakes have occurred on the Hyden Fault during the Quaternary (E1: ca. 20 ka, E2: ca. 50-55 ka, E3: ca. 100 ka, and two events E4 and E5, >200 ka). Activity is highly episodic and slip rates vary from less than 0.01 mm/yr to 0.03 mm/yr for the three seismic cycles for which we have constraint. Palaeo-earthquake magnitudes are estimated to range up to M 6.8. That relief has been preserved relatively unchanged for this length of time is remarkable, and indicates extreme landscape stability.

Acknowledgements

We are indebted to Mike Machette and Tony Crone of the USGS for providing us access to their field data, and for stimulating discussion. Mark Douthie is thanked for allowing us access to his land, upon which our trench was excavated. The Department of Land Information in Western Australia is thanks for providing access to their landmonitor digital elevation data. This research is published with the permission of the CEO of Geoscience Australia, and was funded by a UWA Grant Scheme award to Mike Dentith.

References

ANAND R.R. AND PAIN M., 2002, Regolith Geology of the Yilgarn Craton, Western Australia: implications for exploration: *Australian Journal of Earth Sciences*, v. 49, p. 3-162.

CHIN R.J., HICKMAN A.H., AND THOM R. 1984. Hyden 1:250 000 scale geological series sheet explanatory notes. *Geological Survey of Western Australia* 21p.

CLARK D J AND LEONARD M. 2003. Principal stress orientations from multiple focal plane solutions: new insight in to the Australian intraplate stress field. (eds Hillis, R.R. & Muller, D.), *Evolution and dynamics of the Australian Plate, G.S.Australia and G.S.America, Joint Special Publication 22*, 91-105.

CLARK D.J. AND MCCUE K. 2003. Australian palaeoseismology: towards a better basis for seismic hazard estimation. *Annales Geophysicae* **46**, 1087-1105.

CRONE A J AND LUZA K V. 1990. Style and timing of Holocene surface faulting on the Meers Fault, southwestern Oklahoma. *Geological Society of America Bulletin* **102**, 1-17.

CRONE A J, DE MARTINI P M, MACHETTE M N, OKUMURA K, AND PRESCOTT J R. 2003. Paleoseismicity of aseismic Quaternary faults in Australia: Implications for fault behaviour in stable continental regions: *Bulletin of the Seismological Society of America* **93**, 1913-1934.

CRONE A J, MACHETTE M N, AND BOWMAN J R. 1997. Episodic nature of earthquake activity in stable continental regions revealed by palaeoseismicity studies of Australian and North American Quaternary faults. *Australian Journal of Earth Sciences* **44**, 203-214.

DENHAM, D., 1988. Australian Seismicity – The puzzle of the not-so-stable continent. *Seismological Research Letters* **59**, 235-240.

DENTITH M.C. AND FEATHERSTONE W.E. 2003. Controls on intra-plate seismicity in southwestern Australia: *Tectonophysics* **376**, 167-184.

DOYLE H.A. 1971. Seismicity and structure in Australia: *Bulletin of the Royal Society of New Zealand* **9**, 149-152.

FRANKEL A, MUELLER C, BARNHARD T, PERKINS D, LEYENDECKER E V, DICKMAN N, HANSON S, AND HOPPER M. 1996. National Seismic Hazard Maps, June 1996 Documentation. *U.S. Geological Survey Open File Report* **96532**.

GORDON F R AND LEWIS J D. 1980. The Meckering and Calingiri earthquakes October 1968 and March 1970. *Western Australia Geological Survey Bulletin* **126**, 229p.

HEMPHILL-HALEY M.A. AND WELDON R.J. 1999. Estimating prehistoric earthquake magnitude from point measurements of surface rupture. *Bulletin of the Seismological Society of America* **89**, 1264-1279.

HILLIS R.R. AND REYNOLDS S.D. 2000. The Australian stress map: *Journal of the Geological Society of London* **157**, 915-921.

JOHNSTON A.C., COPPERSMITH K.J., KANTER L.R. AND CORNELL C.A. 1994. The earthquakes of stable continental regions: *Electric Power Research Institute Report*. **TR102261V1**.

LEWIS J D, DAETWYLER N A, BUNTING J A, AND MONCRIEFF J S. 1981. The Cadoux earthquake: *Western Australia Geological Survey Report* **1981/11**, 133p.

MACHETTE M.N. 1998. Contrasts between short- and long-term records of seismicity in the Rio Grande Rift: important implications for seismic hazard assessments in areas of slow extension: *Utah Geological Survey Miscellaneous Publication* **98-2**, 84-95.

MCCUE K. 1990. Australia's large earthquakes and Recent fault scarps: *Journal of Structural Geology* **12**, 761-766.

SALAMA R.B. 1997. Geomorphology, geology and palaeohydrology of the broad alluvial valleys of the Salt River System, Western Australia: *Australian Journal of Earth Sciences* **44**:751-765.

SANDIFORD M, 2003a. Neotectonics of southeastern Australia: linking the Quaternary faulting record with seismicity and in situ stress: In: eds Hillis R.R. & Muller D, Evolution and dynamics of the Australian Plate, *Geological Society of Australia Special Publication* **22**, 101-113.

STIRLING M.W., McVERRY G.H. AND BERRYMAN K.R. 2002. A new seismic hazard model for New Zealand: *Bulletin of the Seismological Society of America* **92**, 1878-1903.

STIRLING M.W., WESNOUSKY S.G., AND BERRYMAN K.R. 1998. Probabilistic seismic hazard analysis of New Zealand: *New Zealand Journal of Geology and Geophysics* **41**, 355-375.

WELLS D L. AND COPPERSMITH K J. 1994. New Empirical relationships among magnitude, rupture length, rupture width, rupture area, and surface displacement. *Bulletin of the Seismological Society of America* **84**, 974-1002.

WILDE, S. A., MIDDLETON, M. F., AND EVANS, B. J. 1996. Terrane accretion in the southwest Yilgarn Craton: evidence from a deep seismic crustal profile: *Precambrian Research* **78**, 179-196.

Figure Captions

Fig. 1 Australian seismicity and fault scarps (after Clark & McCue, 2003).

This map seems to contain a lot of unnecessary details. What it could benefit from is a terrain model as the underlay to emphasis a key aspect of the Introd – i.e. much seismicity, little relief etc.

Fig. 2 Large scale structure and geology of the southwest Yilgarn Craton (after Wilde et al.,1996). Earthquake epicentres from the Geoscience Australia earthquake catalogue (current to May 2005) and Quaternary fault scarps (from Clark & McCue, 2003) are superposed.

Fig. 3 Context of the Hyden Fault scarp. a) scarps and lineaments derived from DEM and airphoto interpretation overlaid onto 1:250,000 scale drainage and geology (after Chin et al., 1984). b) topography of the scarps expressed in the DLI 10 m DEM. Trench locations from this and previous studies are marked. Abbreviations: AN = AGSO north trench, AC = AGSO central trench, AS = AGSO south trench, US = USGS trench.

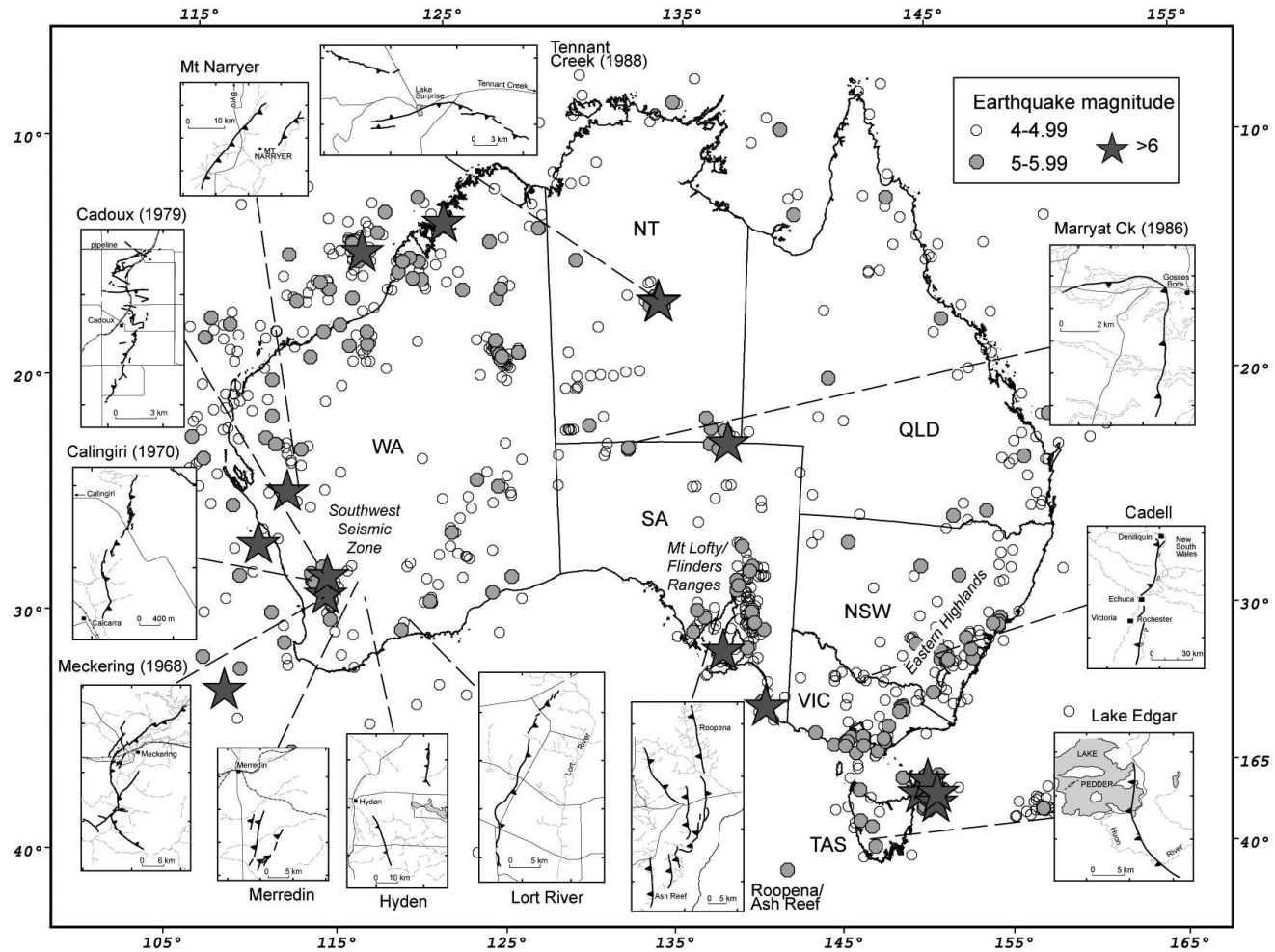
Fig. 4 Log of the southern wall of the trench excavated across the Hyden Fault scarp. Location of trench as marked on **Fig. 3**. Caption needs expanding.

Fig. 5 Cartoon depicting the inferred evolution of structures and sedimentary units within the trench (ie. retro-deformation analysis). Numbers marked on part a) are OSL ages as given in **Table 1**.

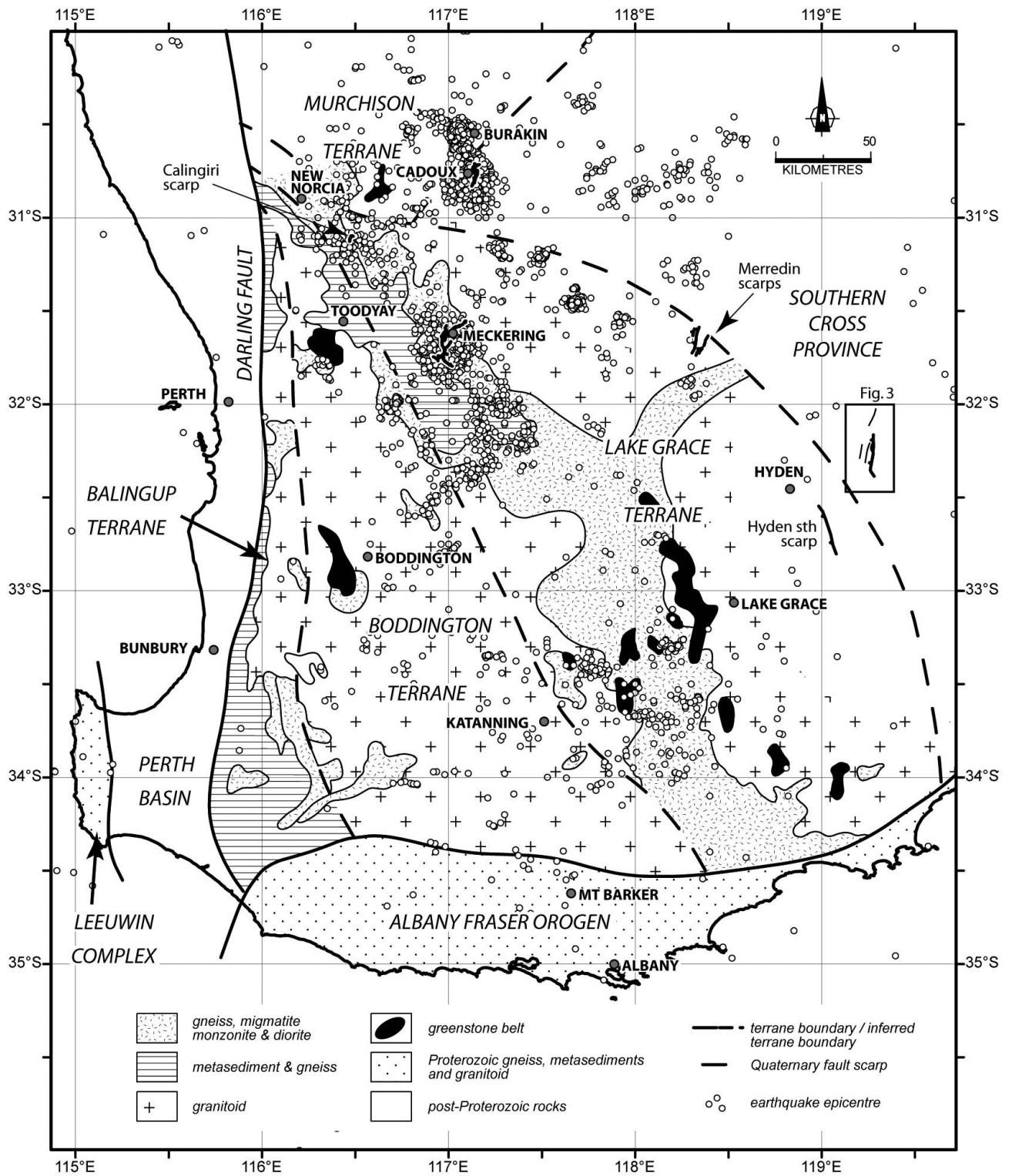
Fig. 6 Compilation diagram of palaeoseismicity data on the Hyden Fault. Right hand column contains slip rate information.

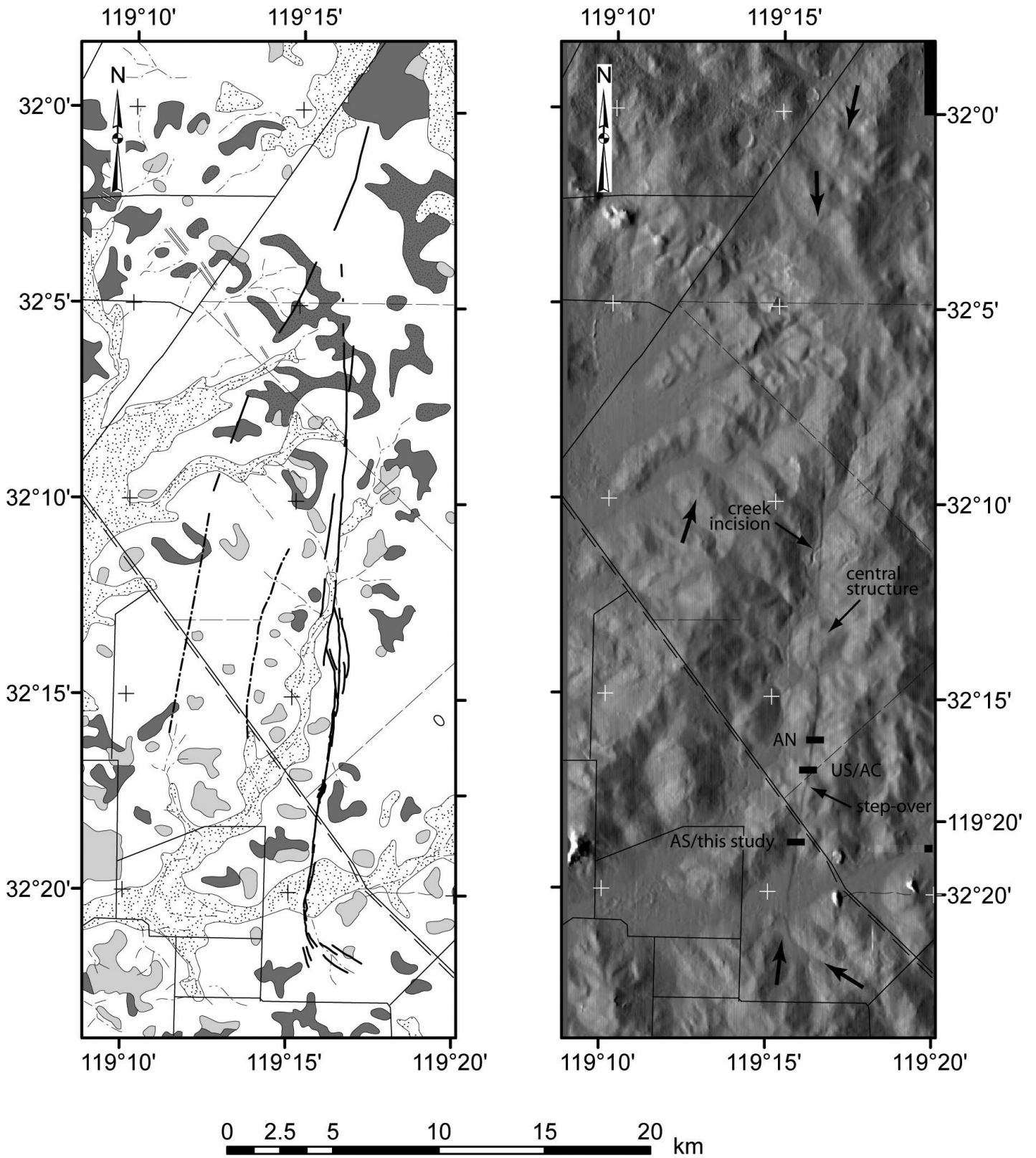
Appendix 1 - OSL analytic techniques.

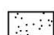








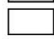
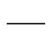
Clark et al.
Fig. 1

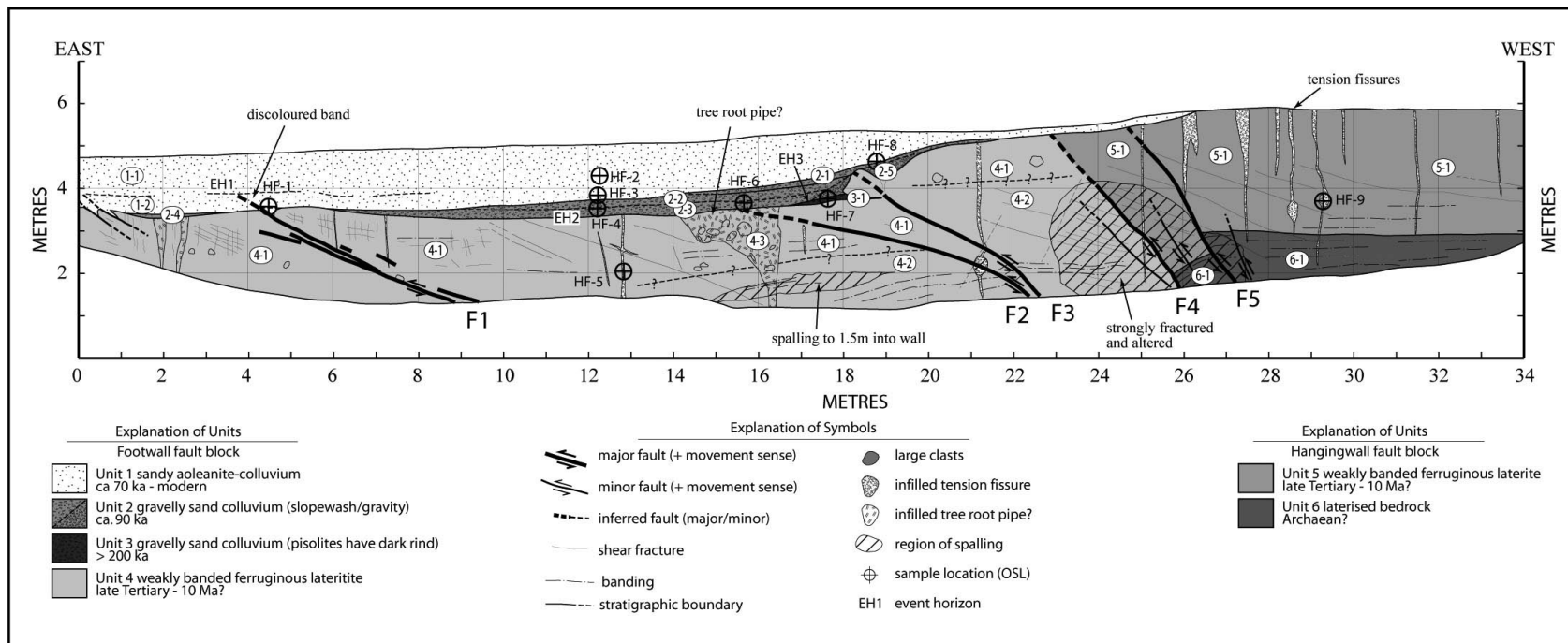


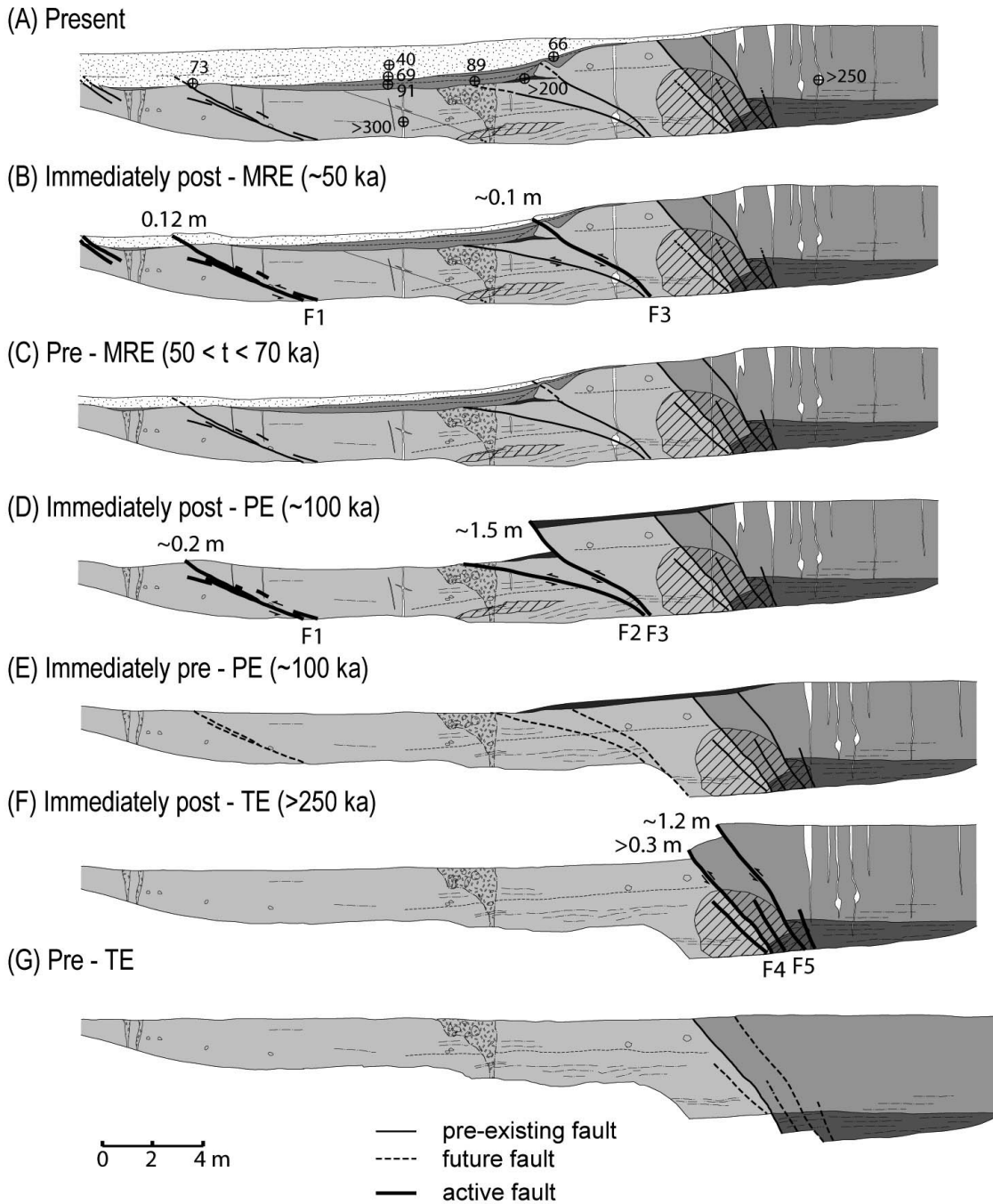
Clark et al.
Fig. 2

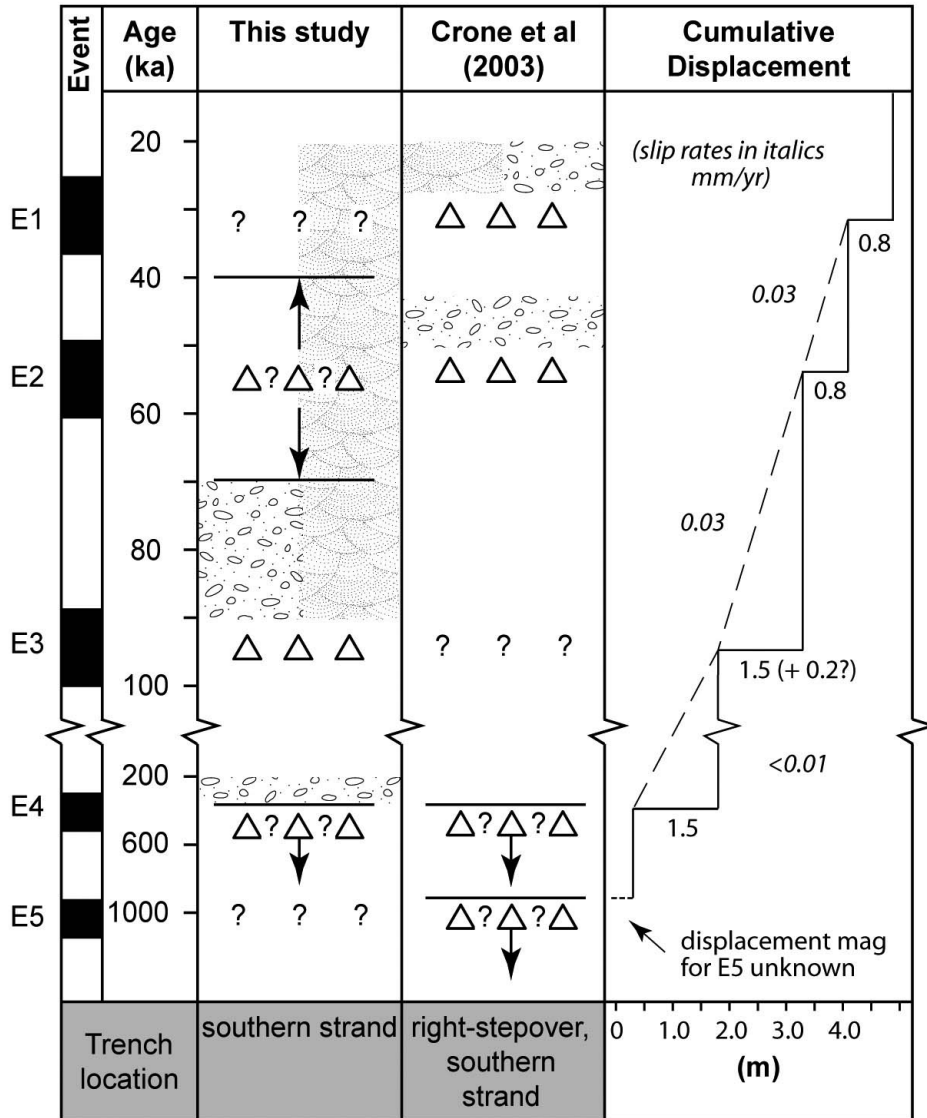









- | | | |
|---|---|--|
|  Quaternary alluvium |  banded iron formation |  track |
|  duricrust (ferricrete/silcrete) |  fault scarp |  stream |
|  granitoid/granitoid gneiss |  airphoto lineament |  trench |
|  sandplain |  formed road | |







-  aeolian deposition
-  colluvial deposition
-  earthquake event (tight age constraint)
-  earthquake event (broad age constraint)
-  event not recognised